

The gain–elevation correction of the IRAM 30–m telescope

A. Greve¹, R. Neri¹, and A. Sievers²

¹ IRAM, 300 rue de la Piscine, 38406 St. Martin d’Hères, France

² IRAM, Nucleo Central, Avda. Divina Pastora 7, 18012 Granada, Spain

Received February 9; accepted May 6, 1998

Abstract. The residual surface deformations of an optimized homologous radio reflector produce an elevation dependent gain variation for which astronomical observations must be corrected. For the IRAM 30–m telescope we provide information, and an example, how to correct observations of point–like and extended sources.

We find agreement between the gain–elevation dependence predicted from the finite element structural calculations and radiometric measurements on the telescope.

Key words: telescopes

1. Introduction

The IRAM 30–m telescope (Baars et al. 1987, 1994) is a homologous construction (von Hoerner 1967a,b) so that for all elevation angles (ϵ) the best–fit reflector surface is a paraboloid. The homology does not eliminate the gravity deformations of the reflector [$\delta_g(i,\epsilon)$ for the surface elements $i = 1, 2, \dots, N$]; however, the root mean square (rms) value σ of the surface deformations of the best–fit parabolic reflector is

$$\sigma(\epsilon) = \sqrt{\sum_i \delta_g(i,\epsilon)^2 / N} \lesssim \lambda_{\min} / 15 \text{ to } \lambda_{\min} / 20 \quad (1)$$

for all elevation angles ($0^\circ \leq \epsilon \leq 90^\circ$) and wavelengths $\lambda_{\min} \leq \lambda$, with λ_{\min} the shortest wavelength of observation of the telescope. If at the elevation angle ϵ_0 the special adjustments $-\delta_g(i,\epsilon_0)$ are applied on the reflector surface, then (von Hoerner & Wong 1975) the reflector is free of gravity deformations at ϵ_0 ($= 43^\circ$ for the 30–m telescope) and the rms–value of the residual surface deformations is

$$\sigma_g(\epsilon) = \sqrt{\sigma(0)^2 [\cos\epsilon - \cos\epsilon_0]^2 + \sigma(90)^2 [\sin\epsilon - \sin\epsilon_0]^2} \quad (2)$$

with $\sigma_g(\epsilon_0) = 0$, and $\sigma(0)$ and $\sigma(90)$ (see below) the gravity induced deformations at horizon ($\epsilon = 0^\circ$) and zenith ($\epsilon = 90^\circ$). The elevation–dependent surface deformations

$\sigma_g(\epsilon)$ introduce an elevation–dependent loss of gain for which astronomical observations must be corrected. The rms–values $\sigma_g(\epsilon)$ are derived from finite element (FE) calculations of the reflector backstructure or from radiometric measurements of astronomical sources. We use both methods and explain, in particular, the gain–elevation dependence as function of the source diameter (θ_s). We provide information how to correct observations made with the 30–m telescope. (See Baars et al. (1987) for an earlier emphasis that a gain–elevation must be applied, at least at short wavelength.)

2. The gain–elevation dependence $G(\epsilon, \epsilon_0)$

Following Ruze’s (1966) antenna tolerance theory, the normalized elevation–dependent **on–axis** antenna gain of the reflector optimized at ϵ_0 is

$$G(\epsilon, \epsilon_0) = \exp[-(4\pi R\sigma_g(\epsilon)/\lambda)^2] \quad (3)$$

where the factor R ($\approx 0.8 - 0.9$) takes into account the steepness of the reflector and the illumination taper of the receiver so that $R\sigma_g$ is the radio–effective surface deformation (Greve & Hooghoudt 1981). The function $G(\epsilon, \epsilon_0)$ depends exclusively on the construction–specific values $\sigma_g(\epsilon)$ which do not change with time and surface adjustment. The homology–corrected telescope–independent flux [S] of a source is obtained from its calibrated flux [$S'(\epsilon)$] measured at the elevation ϵ by application of the correction $G^{-1}(\epsilon, \epsilon_0)$ so that¹

$$S = S'(\epsilon) G^{-1}(\epsilon, \epsilon_0). \quad (4)$$

The literature does not provide explicit information how to deal with extended sources. We will show that for the specific case of the IRAM 30–m telescope, the on–axis

¹ At the 30–m telescope, this correction is *not* automatically applied to observations with heterodyne receivers (3 mm – 0.8 mm); for this use Table 2 and Fig. 3. An example is given below. The correction *is* applied to on–off measurements and *can be applied optionally* to mapping observations with the 230 GHz bolometer when the NIC reduction package is used.

Table 1. Beamwidth θ_b of the 30-m telescope for receivers of ~ -13 dB edge taper, and the largest source diameter θ^* [planet] suitable for determination of the gain–elevation dependence at the specific wavelength

Wavelength	Frequency	θ_b	θ^*	
3 mm	100 GHz	24.0''	$\sim 50''$	Jupiter
2 mm	150 GHz	16.0''	$\sim 30''$	Saturn
1.3 mm	230 GHz	10.4''	$\sim 20''$	Mars
0.86 mm	350 GHz	8.3''	$\sim 15''$	Mars

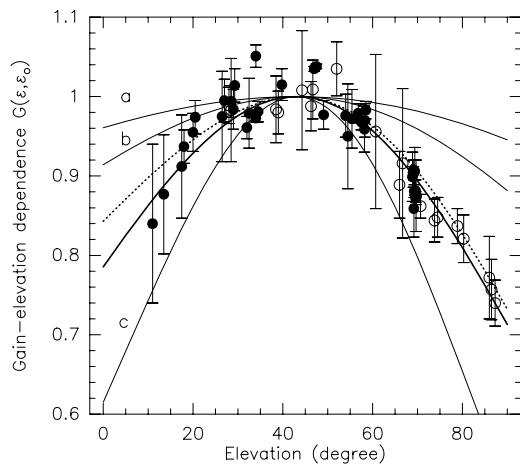


Fig. 1. Gain–elevation dependence measured with the MPIFR bolometer at 1.22 mm (245 GHz) on the quasar 0932+392 [open circles] and Mars (14'') [dots] (Feb. 1995). The heavy line shows the best–fit gain–elevation dependence Eq. (3) derived from these measurements; the dashed line shows the corresponding gain–elevation dependence derived for the surface deformations predicted from the finite element calculations. The other lines show the gain–elevation dependence at 3 mm (100 GHz): **a**), 2 mm (150 GHz): **b**), and 0.86 mm (350 GHz): **c**), derived from scaling of the 1.22 mm gain–elevation dependence (heavy line)

gain–elevation dependence $G(\epsilon, \epsilon_0)$ holds also for extended sources not exceeding in diameter approximately two half–power beamwidths (i.e. $\theta_S \lesssim 2\theta_b$); a weaker gain–elevation dependence applies for more extended sources (i.e. $2\theta_b < \theta_S$). The half–power beamwidth (FWHP) of the 30-m telescope is $\theta_b = 1.16 \lambda/D$ [rad], with λ the wavelength of observation and D the diameter of the reflector; the relevant beamwidths are given in Table 1. Note that the diameter of the full beam is $\sim 2.4\theta_b$.

3. Measurement and calculation of $G(\epsilon, \epsilon_0)$

3.1. Measurement of $G(\epsilon, \epsilon_0)$

The experimental determination of $G(\epsilon, \epsilon_0)$, and $\sigma_g(\epsilon)$, is preferentially made at short wavelengths despite the higher atmospheric noise and less precise atmospheric correction, in particular at low elevations. Figure 1 shows the gain–elevation dependence at 1.22 mm wavelength

obtained from on–off measurements (30'' wobbler throw) with the MPIFR bolometer of the quasar 0923+392 and the extended source Mars (14'' diameter). The bolometer has a taper of ~ -10 dB, a bandwidth of $\Delta\nu \approx 60$ GHz, and for observations of the planets an effective wavelength $\lambda_{\text{eff}} \approx 1.22$ mm (245 GHz), as calculated from the spectral energy distribution of the planets and the wavelength dependent atmospheric attenuation. Figure 1 shows also the gain–elevation dependence calculated from Eq. (2) and Eq. (3) for the best–fit values $\sigma(0) = 0.085$ mm and $\sigma(90) = 0.075$ mm derived from the lsq–fit of the 245 GHz bolometer measurements, using $R = 0.9$. The figure shows furthermore the gain–elevation dependence derived from the FE calculations. Comparison of these curves shows that the rms–values $\sigma_g(\epsilon)$ predicted from the FE calculations are $\sim 10 - 15\%$ lower than those derived from the radiometric measurements.

Inserted in Fig. 1 is the gain–elevation dependence for 3 mm (100 GHz), 2 mm (150 GHz), and 0.86 mm (350 GHz) wavelength, derived from scaling of the empirical 1.22 mm gain–elevation dependence by using the best–fit values $\sigma(0)$ and $\sigma(90)$ in Eq. (2) and Eq. (3).

3.2. Calculation of $G(\epsilon, \epsilon_0)$

In a diffraction calculation we derived the illumination weighted beam patterns $\mathcal{F}(\theta_A, \theta_\epsilon, \epsilon)$ (θ_A = azimuth direction, θ_ϵ = elevation direction) degraded by the wavefront deformation of the homology deformations $\delta_g(\epsilon)$ predicted from the FE calculations², which were scaled in amplitude by $\sim 10 - 15\%$ to match the empirical values $\sigma_g(\epsilon)$. As example, Fig. 2 shows for several elevation angles the calculated beam pattern at $\lambda = 1.30$ mm (230 GHz), i.e. at the wavelength of the $^{12}\text{CO}(2-1)$ line. From these and similar beam patterns we calculated for disk–like and constant surface brightness sources of diameter θ_S [$\Pi(\theta_A, \theta_\epsilon) = 1$ for $\theta_A^2 + \theta_\epsilon^2 \leq (\theta_S/2)^2$ and $\Pi(u, v) = 0$ for $(\theta_S/2)^2 < \theta_A^2 + \theta_\epsilon^2$] the received power

$$\mathcal{P}(\epsilon, \theta_S) = \int \int_{\theta(S)} \mathcal{F}(\theta_A - \theta'_A, \theta_\epsilon - \theta'_\epsilon, \delta_g(\epsilon)) \Pi(\theta'_A, \theta'_\epsilon) d\theta'_A d\theta'_\epsilon \quad (5)$$

and the corresponding gain–elevation dependence

$$G(\epsilon, \epsilon_0, \theta_S) = \mathcal{P}(\epsilon, \theta_S) / \mathcal{P}(\epsilon_0, \theta_S). \quad (6)$$

Table 2 summarizes the **on–axis** gain–elevation dependence $G(\epsilon, \theta_S = 0) \equiv G_0(\epsilon)$ derived from the diffraction calculations, and to be applied on the IRAM 30-m telescope for observations at $\lambda = 3$ mm (100 GHz), 2 mm (150 GHz), 1.30 mm (230 GHz), and $\lambda = 0.86$ mm (350 GHz). For an estimated error of $\pm 10\%$ in the values $\sigma_g(\epsilon)$, the accuracy of the values G_0 is $\pm 2\%$ at long wavelengths (3 mm – 2 mm) and $\pm 5\%$ at short wavelengths

² For contour maps of the homology deformations see Greve et al. (1996).

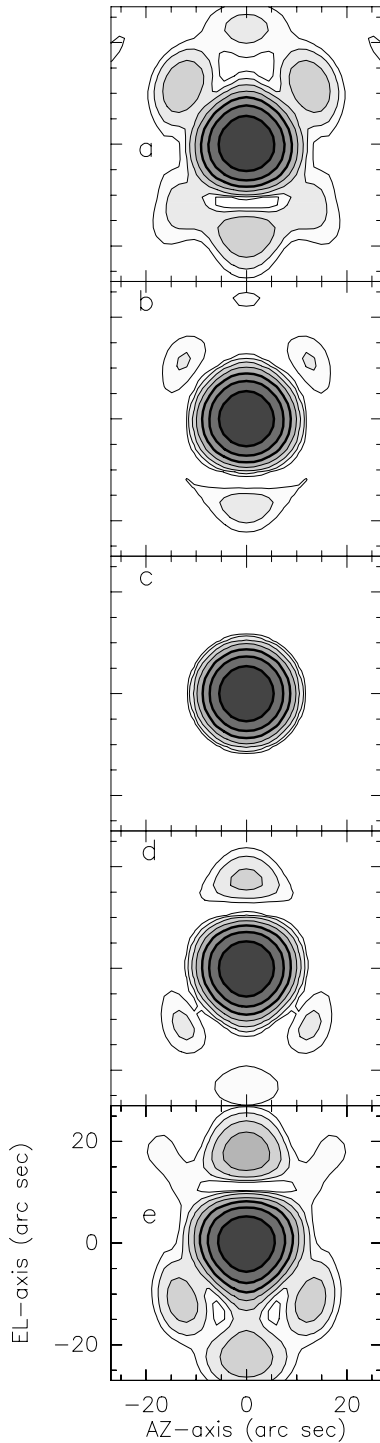


Fig. 2. Beam pattern $\mathcal{F}(\theta_A, \theta_\epsilon, \epsilon)$ of the IRAM 30–m telescope calculated for $\lambda = 1.30$ mm (230 GHz) and the elevation angle 0° a), 22.5° b), 43° c), 67.5° d), and 90° e). The reflector is optimized at $\epsilon_0 = 43^\circ$ so that at this elevation the calculated reference beam is the perfect beam pattern. Heavy contours: levels at -3 dB, -6 dB, and -9 dB; thin contours: levels at -12 dB, -15 dB, -18 dB, and -21 dB

Table 2. On-axis gain–elevation dependence $G_0(\epsilon, \epsilon_0)$ for $\lambda = 3$ mm (100 GHz), 2 mm (150 GHz), 1.3 mm (230 GHz), and 0.86 mm (350 GHz) [receivers of ~ -13 dB edge taper]. The accuracy of σ_g and $R\sigma_g$ is $\sim \pm 10\%$

Elevat.	σ_g	$R\sigma_g$	G_0	G_0	G_0	G_0
[degr]	$[\mu\text{m}]$	$[\mu\text{m}]$	3 mm	2 mm	1.3 mm	0.86 mm
0	55	52	0.95	0.88	0.77	0.55
10	45	40	0.97	0.92	0.85	0.69
20	31	30	0.98	0.95	0.92	0.83
30	18	17	0.99	0.98	0.97	0.94
40	4	4	1.00	1.00	0.99	0.99
43	0	0	1.00	1.00	1.00	1.00
50	10	9	1.00	1.00	0.99	0.98
60	25	22	0.99	0.98	0.95	0.90
70	38	35	0.98	0.95	0.89	0.77
80	52	46	0.96	0.92	0.82	0.63
90	65	57	0.94	0.88	0.74	0.50

(1.3 mm – 0.8 mm). As evident from Fig. 1 and Table 2, the gain–elevation dependence at 3 mm wavelength is only a few percent and usually below the accuracy of the measurements. The small difference between the curves of Fig. 1 and the data of Table 2 is due to the empirical determination and the calculation of $G(\epsilon, \epsilon_0)$; however, the difference is below the accuracy of the measurements.

An extended source is covered by a larger fraction of the beam than a point–source and hence should show a smaller gain–elevation dependence. To quantify this effect, we use the loss in gain

$$L(\epsilon, \theta_S) = 1 - G(\epsilon, \theta_S) \quad (7)$$

and display in Fig. 3 the relative loss in gain $\mathcal{L}(\epsilon, \theta_S)$ between a point–source ($L(\epsilon, 0)$) and an extended source ($L(\epsilon, \theta_S)$) calculated from

$$L(\epsilon, \theta_S)/L(\epsilon, 0) = \mathcal{L}(\theta_S). \quad (8)$$

The calculations show as important result that the quantity $\mathcal{L}(\theta_S)$ is nearly independent of the wavelength and the elevation of the observation³. Using the data of Fig. 3 and the entries of Table 2, the actual value $G(\epsilon, \epsilon_0, \theta_S)$ for an extended source is

$$G(\epsilon, \epsilon_0, \theta_S) = 1 - \mathcal{L}(\theta_S) L(\epsilon, 0) = 1 - \mathcal{L}(1 - G_0). \quad (9)$$

Figure 3 shows that $0.95 \lesssim \mathcal{L}(\theta_S)$ for sources not exceeding $\theta_S \lesssim 2\theta_b$ so that from Eq. (9) for these sources $G(\theta_S) \approx G_0$, within 5 – 10%. The gain–elevation dependence is weaker for more extended sources since for these $\mathcal{L}(\theta_S) < 0.9$. The gain–elevation dependence is negligible for sources of diameter $8\theta_b \lesssim \theta_S$ since for these $\mathcal{L}(\theta_S) \lesssim 0.1$ and $G(\theta_S) \approx 1$.

We explain in the following example how to correct observations with the 30–m telescope. Suppose a source

³ This result is explained from the fact that the homology deformations can be expressed as a fixed set of elevation–scaled Zernike polynomials and additional random errors (see Greve et al. 1996).

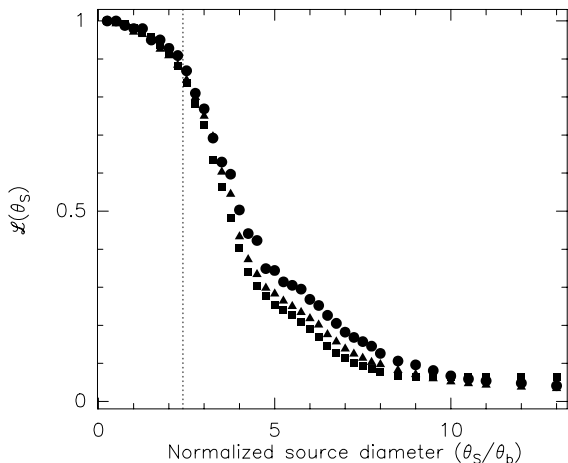


Fig. 3. Relative gain–elevation dependence $\mathcal{L}(\theta_S)$ (Eq. (8)) as function of source size θ_S (in units of beamwidth θ_b), for $\lambda = 2.0$ mm (150 GHz): triangles, $\lambda = 1.30$ mm (230 GHz): squares, $\lambda = 0.86$ mm (350 GHz): circles. The dashed vertical line indicates the diameter of the full beam $\sim 2.4\theta_b$, i.e. the position of the first minimum

of $\theta_S = 30''$ diameter, observed at 1.3 mm wavelength and 20° elevation, has a flux corrected for atmospheric attenuation of $S'(\epsilon = 20^\circ) = (2 \text{ k/A}) F_{\text{eff}} T_A^*/\epsilon_{\text{ap}} = 10$ Jy. The diameter of the source is $30''/\theta_b \approx 3$ beamwidth. From Fig. 3 we find $\mathcal{L}(3) = 0.70$, so that from Eq. (9) and the value $G_0(20^\circ) = 0.92$ of Table 2 we have $G(30'') = 1 - 0.70(1 - 0.92) = 0.94$. The homology–corrected telescope–independent flux is $S = S'(20^\circ)/0.94 = 10.6$ Jy. A 10 Jy point–source observed under similar conditions has the intrinsic flux $S = 10/0.92 = 10.9$ Jy.

4. Summary

We find for the IRAM 30–m telescope that

(1) there is agreement within 10 – 15% between the rms–values $\sigma_g(\epsilon)$ derived from the radiometric measurements and the finite element calculations (see Fig. 1). This accuracy is set by the radiometric measurements and the atmospheric correction, rather than by the accuracy of the FE structural calculations.

(2) Figure 3 indicates that the on–axis gain–elevation dependence $G_0(\epsilon, \epsilon_0)$ holds for extended sources not exceeding in diameter approximately two half–power beamwidths ($\theta_S \lesssim 2\theta_b$), i.e. approximately the diameter of the main beam. This result implies that the gain–elevation dependence can be determined without correction from the measurement of extended sources, for instance the planets, in case they do not exceed $2\theta_b \equiv \theta^*$. Table 1 gives the values θ^* and largest planet suitable for determination of the gain–elevation dependence. As evident from Fig. 3, the gain–elevation dependence decreases for sources larger than two beamwidths and disappears for sources larger than ~ 8 beamwidths.

(3) for any wavelength in the range $0.8 \text{ mm} \lesssim \lambda \lesssim 3 \text{ mm}$, the **on–axis** gain–elevation dependence G_0 is obtained from Eq. (3) using the radio–effective rms–values $R\sigma_g(\epsilon)$ of Table 2. The gain–elevation dependence for extended sources is obtained from these values and the data of Fig. 3, using Eq. (9).

Acknowledgements. The homology calculations were originally made by ARGE KRUPP (now VERTEX) and MAN, Germany, and later repeated by P. Raffin (formerly at IRAM) and M. Bremer (IRAM). We profited from many discussions with our colleagues in the effort to measure a reliable gain–elevation curve. We thank the referee, Mr. J. Baars, for his comments and his Occam razor.

References

- Baars J.W.M., Hooghoudt B.G., Mezger P.G., de Jonge M., 1987, A&A 175, 319
- Baars J.W.M., Greve A., Hein H., et al., 1994, Proc. IEEE 82, 687
- Greve A., Hooghoudt B.G., 1981, A&A 93, 76
- Greve A., Baars J.W.M., Penalver J., LeFloch B., 1996, Radio Sci. 31, 1053
- Ruze J., 1966, Proc. IEEE 54, 633
- von Hoerner S., 1967a, J. Struct. Div. Amer. Soc. Civil Eng. 83, 461
- von Hoerner S., 1967b, AJ 72, 35
- von Hoerner S., Wong W–Y., 1975, Trans. IEEE Ant. Propagat. AP–23, 689